Journal of
Medical Genetics

A novel form of rhizomelic skeletal dysplasia associated with a homozygous variant in GNPNAT1

Journal:	*Journal of Medical Genetics*
Manuscript ID	jmedgenet-2020-106929.R2
Article Type:	Original research
Date Submitted by the Author:	n/a
Keywords:	Genetics, Molecular genetics, Cell biology

Complete List of Authors:
Ain, Noor; University of the Punjab, School of Biological Sciences
Baroncelli, Marta; Karolinska Institute, Center for Molecular Medicine and Pediatric Endocrinology Unit, Department of Women's and Children's Health
Costantini, Alice; Karolinska Institutet Department of Molecular Medicine and Surgery,
Ishaq, Tayyaba ; University of the Punjab, School of Biological Sciences
Taylan, Fulya; Karolinska Institutet, Molecular Medicine and Surgery
Nilsson, Ola; Karolinska Institute, Center for Molecular Medicine and Pediatric Endocrinology Unit, Department of Women's and Children's Health
Mäkitie, Outi; University of Helsinki, Children's hospital
Naz, Sadaf; University of the Punjab, School of Biological Sciences

A novel form of rhizomelic skeletal dysplasia associated with a homozygous variant in *GNPNAT1*

Noor ul Ain[1,2], Marta Baroncelli[3], Alice Costantini[2], Tayyaba Ishaq[1], Fulya Taylan[2], Ola Nilsson[3,4], Outi Makitie[2,5,6]*, Sadaf Naz[1*]

[1]School of Biological Sciences, University of the Punjab, Lahore, Pakistan

[2]Department of Molecular Medicine and Surgery and Center for Molecular Medicine, Karolinska Institutet, Stockholm, Sweden

[3]Center for Molecular Medicine and Pediatric Endocrinology Unit, Department of Women's and Children's Health, Karolinska Institutet and University Hospital, Stockholm, Sweden

[4]School of Medical Sciences, Örebro University and Örebro University Hospital, Örebro, Sweden

[5]Folkhälsan Institute of Genetics, Helsinki, Finland

[6]Children's Hospital, University of Helsinki and Helsinki University Hospital, Helsinki, Finland

Noor ul Ain's current address: Institute of Biomedical and Genetic Engineering, Islamabad, Pakistan

*OM, SN equal contribution

Correspondence to

Dr. Outi Makitie

Children's Hospital, P.O. Box 281, Helsinki University Hospital, FI-00027 Helsinki, Finland

outi.makitie@helsinki.fi

Dr. Sadaf Naz,

School of Biological Sciences, University of the Punjab

Quaid-i-Azam Campus, Lahore, 54590, Pakistan

naz.sbs@pu.edu.pk

Abstract

Background: Studies exploring molecular mechanisms underlying congenital skeletal disorders have revealed novel regulators of skeletal homeostasis and shown protein glycosylation to play an important role.

Objective: To identify the genetic cause of rhizomelic skeletal dysplasia in a consanguineous Pakistani family.

Methods: Clinical investigations were carried out for four affected individuals in the recruited family. Whole genome sequencing (WGS) was completed using DNA from two affected and two unaffected individuals from the family. Sequencing data were processed, filtered and analyzed. *In silico* analyses were performed to predict the effects of the candidate variant on the protein structure and function. Small interfering RNAs (siRNAs) were used to study the effect of *Gnpnat1* gene knockdown in primary rat chondrocytes.

Results: The patients presented with short stature due to extreme shortening of the proximal segments of the limbs. Radiographs of one individual showed hip dysplasia and severe platyspondyly. WGS data analyses identified a homozygous missense variant c.226G>A; p.(Glu76Lys) in *GNPNAT1*, segregating with the disease. Glucosamine 6-phosphate N-acetyltransferase, encoded by the highly conserved gene *GNPNAT1*, is one of the enzymes required for synthesis of uridine diphosphate N-acetylglucosamine, which participates in protein glycosylation. Knockdown of *Gnpnat1* by siRNAs decreased cellular proliferation and expression of chondrocyte differentiation markers collagen type 2 and alkaline phosphatase, indicating that *Gnpnat1* is important for growth plate chondrocyte proliferation and differentiation.

Conclusions: This study describes a novel severe skeletal dysplasia associated with a biallelic, variant in *GNPNAT1*. Our data suggest that GNPNAT1 is important for growth plate chondrogenesis.

Keywords: rhizomelic dysplasia, glycosylation, chondrocyte, whole genome sequencing, Pakistan

Introduction

Skeletal dysplasias are a genetically and clinically heterogeneous group of more than 400 inherited disorders affecting bone and cartilage development or morphology [1]. Although over 350 genes have been characterized in skeletal dysplasias, the genetic defects underlying many of these conditions are still unknown. Skeletal dysplasias can be classified based on clinical features, radiological findings and molecular mechanisms. Several skeletal dysplasias are associated with short stature; such disorders can be further classified based on the most severely affected body parts. Rhizomelic dysplasias are characterized by severe shortening and deformities of the proximal parts of upper (humerus) and lower (femur) limbs.

Studies into molecular mechanisms underlying skeletal dysplasias have elucidated processes that are important for bone homeostasis. Glycosylation, an enzymatic process involving the attachment of glycans to proteins and lipids [2], is a vital process in all cells and is essential for numerous functions, including cellular localization, transport, signaling, and metabolism of proteins and lipids. Nucleotide-activated sugars serve as donors of glycan moieties during glycosylation. Several congenital disorders are caused by pathogenic variants affecting genes that encode proteins involved in glycosylation [3]. So far more than 100 congenital disorders of glycosylation have been described [4] and some of these conditions also feature skeletal anomalies [5].

We describe a consanguineous family with four adults affected by a novel form of severe rhizomelic skeletal dysplasia. Through whole genome sequencing, we identified a biallelic

missense variant in *GNPNAT1* as the likely cause of their disorder. We provide evidence that GNPNAT1 is involved in proliferation and differentiation of chondrocytes.

Subjects and Methods

Ethics Statement

This study was approved by Institutional Review Board of School of Biological Sciences, University of the Punjab, Lahore, Pakistan (Ethics approval SBS11-1 by IRB # 00005281). Written informed consents were obtained from all participants. The animal protocol and all procedures were approved by the regional animal ethics committee in Stockholm, Sweden.

Subjects

A consanguineous Pakistani family NAD-07 with four affected individuals was recruited in the study. We collected a detailed family history about onset and progression of the disorder. Heights of all participating individuals were measured. Photographs of arms, legs and radiographs of forearms, forelegs and spine of individual IV:4 were obtained for phenotypic evaluation. Blood samples were obtained from all participating individuals. DNA was isolated by sucrose lysis and salting out method.

Molecular Analysis

Whole genome sequencing (WGS) was performed for two affected and two unaffected individuals. Libraries were prepared by using Illumina TruSeq PCR-free kit. Pair-end reads with average coverage of 30X were obtained on the HiSeq X instrument (Illumina, CA, USA) at the Science for Life Laboratory (SciLifeLab), Stockholm. The data were processed using our in-

house pipeline. In brief, Burrow-Wheeler Aligner (BWA) [6] was used for mapping reads to the reference human genome (assembly b37). Genome Analysis Toolkit (GATK) [7] was used for duplicate marking, variant calling and joint genotyping. Variants were annotated using Variant Effect Predictor (VEP) [8] and then loaded into a database generated by GEMINI [9]. Rare variants (minor allele frequency <0.01 in publicly available population databases ExAC, gnomAD and SweGen) in the coding sequences and splice sites that supported autosomal recessive inheritance model were prioritized. The variants were further evaluated based on the conservation (GERP) and pathogenicity scores (CADD). The segregation of the variant with the skeletal phenotype was investigated in all family members by Sanger sequencing.

Computational Modeling of mutant protein

Human GNPNAT1 crystal structure was obtained from protein databank (PDB Identifier: 2O28). I-mutant 2.0 (http://folding.biofold.org/i-mutant/i-mutant2.0.html) was used to predict the effect of Glutamic acid to Lysine substitution at position 76 on protein stability.

Chondrocyte isolation and culture

Proximal tibias and distal femurs of 3-5 day old rats (Sprague Dawley, Charles River Laboratory, Wilmington, MA, USA) were obtained after dissection and digested with 0.3% collagenase type IA (Sigma-Aldrich, Darmstadt, Germany) in DMEM/F12 in aseptic conditions as previously described [10]. Dissected cartilage pieces were washed twice in PBS with 1% penicillin/streptomycin, 50 ng/ml fungizone (all by Thermo Fisher Scientific, Waltham, MA, USA), followed by incubation in 0.1% EDTA (Sigma-Aldrich, Darmstadt, Germany) in PBS for 15 minutes, and eventually 0.125% trypsin (Thermo Fisher Scientific) in PBS for 30 minutes, at

37°C in shaking conditions. Cartilage pieces were subsequently washed twice in PBS with 1% penicillin/streptomycin, 50ng/ml fungizone, and digested with 0.3% collagenase type IA (Sigma-Aldrich) in DMEM/F12 at 37°C while shaking. Cycles of 30 minutes were repeated until digestion was complete. The resulting cell suspension was filtered through 70µm-cell strainer (BD Biosciences, San Jose, CA, USA), spun at 300g for 5 minutes and washed twice in PBS with 1% penicillin/streptomycin, 50ng/ml fungizone. The released chondrocytes were cultured in DMEM/F12 with GlutaMAX, with 10% fetal bovine serum (FBS), 50µg/ml ascorbic acid (Thermo Fisher Scientific), 50ng/ml fungizone and 1% penicillin/streptomycin at 37°C, 5% CO_2.

Gnpnat1 siRNA knock-down

In order to determine the impact of *Gnpnat1* knockdown on chondrocytes, two pre-designed small interfering RNAs (siRNA), *Silencer*™ Select siR1 (s176980) and siR2 (s176982), were obtained from Life Technologies® (Thermo Fisher Scientific) and used for knocking down *Gnpnat1* in rat primary chondrocytes. *Silencer*™ Select Negative Control No. 1 siRNA (4390843; Thermo Fisher Scientific) and siRNA against *Gapdh* (4390849; Thermo Fisher Scientific) were used as negative and positive controls, respectively.

Transfection of rat primary chondrocytes with siRNAs

Rat chondrocytes (25000/cm^2) were transfected with *Gnpnat1* specific siRNAs or control siRNAs at 60% confluency, as previously described [11]. One hour prior to transfection, cells were washed with PBS, and culture medium was changed to DMEM/F12 without antibiotics. Chondrocytes were transfected with 40nM of scramble siRNA (4390843), the two siRNAs against *Gnpnat1* (s176980 or s176982) or *Gapdh* siRNA as positive control, according to

manufacturer's protocol, using Lipofectamine 3000 (Thermo Fisher Scientific). Culture medium was replaced with DMEM/F12 with GlutaMAX supplemented with 10% fetal bovine serum (FBS), 50µg/ml ascorbic acid, 1% penicillin/streptomycin, and 50ng/ml fungizone 16 hours post-transfection.

Apoptosis and proliferation assessment

Chondrocyte apoptosis and proliferation were examined 48h post-transfection. Apoptosis was measured by detecting cytoplasmic histone-associated DNA fragments in cell lysates photometrically, according to manufacturer's instructions (Roche, Mannheim, Germany). Briefly, cell lysates were transferred to a streptavidin-coated plate and incubated with biotinylated anti-histones antibodies and anti-DNA antibodies conjugated with peroxidase. Washing steps were used to remove unbound components. The amount of peroxidase retained in the immunocomplex was determined photometrically at 405nm after substrate addition (tetramethyl-benzidine from Roche).

Cell proliferation was measured by colorimetric detection based on incorporation of 5′-bromo-2′-deoxyuridine (BrdU) (Roche) according to the standard protocol. In brief, 48h post-transfection, cells were incubated with BrdU for 3h, and the absorbance was measured at 370nm (SpectraMax Plus 384 Microplate Reader, Molecular Devices LLC, San Jose, CA, USA). As a control for background, incorporation in cells of BrdU was measured after only a few seconds following treatment.

Quantitative real time PCR

Gene expression was assessed 48h post-transfection. Cell lysates were collected in solution C (4M guanidine thiocyanate, 25mM sodium citrate pH7, 0.1M β-mercaptoethanol) and total RNA was extracted using phenol/chloroform [10]. cDNA was synthesized from total RNA (50ng) by Superscript Reverse Transcriptase III (Thermo Fisher Scientific). ABI Prism 7900 Fast Sequence Detector (Thermo Fisher Scientific) was used to quantify the expression of *Gnpnat1*, alkaline phosphatase (*Alpl*) and collagen type 2 (*Col2a1*) using SYBR green. Data were normalized to 18S rRNA and relative gene expression was calculated using the algorithm: $2^{-\Delta Ct} * 10^6$ as previously described [12].

Statistical analysis

All siRNA experiments were performed in triplicates. Values are presented as average ± standard error of the mean (SEM). Unpaired T tests (GraphPad Prism 7.0 (GraphPad Software, Inc., La Jolla, CA, USA) were used to calculate significance of each siRNA-treated sample compared to the scrambled RNA control.

Results

Clinical Presentation

Family NAD-07 has four affected siblings born to consanguineous parents. The father and the only unaffected sister were deceased at the time of ascertainment. All affected individuals were above 40 years of age and the mother was 80 years old. The affected individuals had a similar phenotype including severe short stature (99 cm - 114 cm), disproportionately increased arm length in comparison to trunk length and large hands and feet relative to total heights (Table 1) (Figure 1A-D). There was marked rhizomelic shortening of the limbs. Hand and feet showed

irregularities in metacarpals and metatarsals length (Figure 1A-D). Affected individuals had abnormal gait and reported restricted joint movements accompanied by pain. Cognition was grossly normal as they all adequately responded to questions during the clinical examination and reportedly were gainfully employed. There were no clinical symptoms suggestive of impaired immunity.

Radiographic Findings

Radiographs of an affected individual IV:4 indicated several skeletal anomalies (Figure 2A-2F). Spinal radiographs revealed platyspondyly involving the whole spine (Figure 2C). Radiographs of the upper arms showed short humeri with underdeveloped proximal parts. Pelvic radiograph indicated hip dysplasia with deformed proximal femurs, absent caput femur and short femoral neck. Femurs were short and the metaphyseal regions around the knees were very wide and abnormal in shape (Figure 2A- 2F).

Molecular Investigation

Whole genome sequencing of four family members revealed 21 variants that were homozygous in the affected individuals and heterozygous in the mother with a MAF < 0.01 (Table S1). Of these, only one homozygous exonic variant in *GNPNAT1* c.226G>A; p.(Glu76Lys) was identified after applying filtration criteria. The variant segregated with the disease phenotype in the family. All affected individuals were homozygous for the variant while the mother was heterozygous and the unaffected niece (V:I) was homozygous for the wild-type allele (Figure 3A, 3B). The variant was absent in all public databases including gnomAD and 1000 genomes as well as in 380 ethnically matched control chromosomes. The variant was predicted to be pathogenic by Polyphen2 and MutationTaster with a Combined Annotation Dependent Depletion

(CADD) score of 22. The *GNPNAT1* c.226G>A; p.(Glu76Lys) variant was deposited in LOVD (LOVD# 0000645198).

Results of computational modeling

Computational modeling of the crystal structure of GNPNAT1 predicted a large decrease in stability (DDG Value Prediction, -0.70 Kcal/mol) of the enzyme due to the amino acid substitution at position 76 (p.Glu76Lys).

Chondrocyte apoptosis is unaffected by *Gnpnat1* knockdown

Gnpnat1 expression was decreased by 4.9-fold ($p<0.001$) and 3.3-fold ($p<0.001$) by siR1 and siR2 respectively, 48 hours after transfection, as compared to chondrocytes transfected with scrambled siRNA (Figure 4A). Cell proliferation was significantly reduced in the chondrocytes transfected with siR2 ($p<0.05$), but the reduction did not reach significance in chondrocytes transfected with siR1 (Figure 4B). Chondrocyte apoptosis was not affected by any of the *Gnpnat1* siRNAs 48 hours after transfection (Figure 4C).

Knockdown of *Gnpnat1* induces de-differentiation of chondrocytes

To investigate whether *Gnpnat1* knockdown influences chondrocyte differentiation, we studied the expression levels of chondrocyte marker *Col2a1* and hypertrophic chondrocyte marker *Alpl*. Both *Alpl* expression and *Col2a1* expressions were significantly reduced in chondrocytes transfected by siR1, by 1.6-fold ($p<0.01$) and 2.1-fold ($p<0.001$), respectively (Figure 4D, 4E). *Gnpnat1* knockdown induced chondrocyte de-differentiation, as the expression of chondrocyte differentiation markers was reduced.

Discussion

We describe a novel autosomal recessive skeletal dysplasia in a consanguineous family. A homozygous missense variant c.226G>A; p.(Glu76Lys) in *GNPNAT1* was identified by whole genome sequencing as the likely cause of the disorder in the studied family. The affected individuals had rhizomelic shortening of limbs and severe short stature.

Inside the Golgi complex, the dolichol-pyrophosphate oligosaccharide, which is transferred to nascent proteins, receives its first monosaccharide from uridine diphosphate N-acetylglucosamine (UDP-GalNAc) during N-glycosylation of secretory/membrane protein. Moreover, synthesis of glycosaminoglycans, proteoglycans and glycosylphosphatidylinositol (GPI) anchors also require UDP-GalNAc as the glycan donor. Endogenous UDP-GalNAc is synthesized from N-acetyl-alpha-D-glucosamine 1-phosphate *de novo* or from salvage pathways. The synthesis of UDP-GalNAc is a four-step process and the second step is catalyzed by glucosamine 6-phosphate N-acetyltransferase (GNPNAT1), encoded by *GNPNAT1*. GNPNAT1 is a small dimeric protein localized in the Golgi and endosome membranes.

The dimeric structure of GNPNAT1 is stabilized by salt bridges and interactions between amino acids situated at the interfacing regions of monomers [13]. The charge density at the interface and the binding site further stabilizes the protein structure and its catalytic activity. The glutamic acid residue at position 76, substituted by lysine (p.(Glu76Lys)), is evolutionarily conserved among diverse vertebrate species (Figure 5A). The variant affects the acetyltransferase domain of the enzyme (Figure 5B). Moreover, the change from an acidic amino acid to a basic amino acid affects the charge distribution of the enzyme as well. Therefore, it is likely that the

p.(Glu76Lys) variant will significantly affect the activity and function of this enzyme. The computational modeling also predicted a decreased stability of the enzyme due to the variant.

Among the orthologues, knocking out *Gnpnat1* in *Saccharomyces cerevisiae* is lethal [14] and homozygous null mutants of murine *Gnpnat1* exhibit a generalized reduction of cell proliferation and development of embryos, resulting in death at 7.5 embryonic day [15]. The mutant mouse embryonic fibroblasts also exhibit impaired actin bundles depolymerization and resistance to apoptotic signals. These cellular defects are rescued by feeding cells with exogeneous UDP-GalNAc. [15]. Thus, taken together these results suggest that intracellular UDP-GalNAc deficiency affects apoptotic and proliferation signaling.

Interestingly, genetic variants in *PGM3* (OMIM 172100) encoding the phosphoglucomutase-3, which is involved in the third step of the synthesis of N-acetyl-alpha-D-glucosamine 1-phosphate (UDP-GalNAc), have been identified in a form of autosomal recessive skeletal dysplasia resembling Desbuquois dysplasia (OMIM 251450) [16]. The phenotype of the affected individuals harboring the *GNPNAT1* variant in our family resembles that of the patients with *PGM3* variants, who also feature a rhizomelic shortening of the long bones. However, in our patients with the *GNPNAT1* defect, rhizomelia was more severe, especially in the upper limbs. At least the proband, homozygous for the *GNPNAT1* variant for whom spinal radiographs were available, had severe platyspondyly as reported for the infants with the *PGM3* variants [16]. The shortened femoral necks and severe dysplasia of the proximal femur due to the *GNPNAT1* variant resembles that seen in patients with the *PGM3* variants. However, the proximal femur develops significantly during the first years of life and since all patients with the *PGM3*

mutations were infants at the time of phenotypic description, the effects of these mutations on the adult skeleton are unknown. The affected individuals in our family did not have mid-face hypoplasia as observed for patients harboring *PGM3* variants. The patients with *PGM3* variants were also anemic and had an immune deficiency. Blood chemistry profiles of the affected individuals in our study were not available for comparison but the patients lacked clinical history suggestive of an increased number or severity of infections. Unfortunately, the family in this study lives in a remote area with restricted access to health care and only limited medical data could be obtained. Our search for additional patients with *GNPNAT1* mutations in our own, or international collaborators' databases of exome data from skeletal dysplasia patients, or through Genematcher were not successful.

Two other conditions bear some resemblance to the skeletal dysplasia described here. Autosomal-recessive omodysplasia (OMIM 258315) is characterized by proximally shortened limbs, facial dysmorphism, and severe short stature. Skeletal features include proximal limb shortening with distal tapering of long bones, proximal radioulnar diastasis, and anterolateral dislocation of the radial head. Facial features include frontal bossing, a flat nasal bridge and anteverted nostrils, low set ears, a long philtrum, and frontal capillary hemangiomas. Adult height ranges from -7.0 to -5.5 SD. The disease is caused by point mutations or by larger genomic rearrangements in glypican 6 (*GPC6*) [17]. Although some of the skeletal changes overlap, our patients did not have the facial characteristics of patients with omodysplasia. Second, the heterogeneous group of cases reported as Patterson-Lowry syndrome have features overlapping those of our patients, especially the proximal humeral deformity [18]. The original case, an elderly adult, also showed some platyspondyly but the spinal changes were not as severe

as seen in our patient [19]. Metacarpal shortening, as observed in our patients, has also been described [20]. Recessive inheritance has been suggested [18] but the genetic cause remains unknown; severity varies from early lethality [21] to relatively mild short stature [20].

Knockdown of *Gnpnat1* in rat primary chondrocytes provided support for the importance of *Gnpnat1* in chondrogenesis. Knockdown of *Gnpnat1* using siRNA significantly decreased proliferation and expression of chondrogenic marker genes *Col2a1* and *Alpl*. These results suggested that *Gnpnat1* is necessary for proliferation and differentiation of chondrocytes; two crucial processes during skeletal formation and growth. Interestingly, siRNA knockdown of *Gnpnat1* did not induce apoptosis in primary rat chondrocytes, thus suggesting that *Gnpnat1* is not necessary to prevent apoptosis. Our findings of decreased chondrocyte proliferation with *Gnpnat1* knockdown, taken together with the previous findings of reduced fibroblasts proliferation in *Gnpnat1* deficient mice [15] may suggest that *Gnpnat1* has an important function during cell proliferation in several cell types, not just chondrocytes. The mechanism for this role is not currently understood and needs to be addressed in future studies.

In summary, these findings broadly support the hypothesis that GNPNAT1 has an important role during formation and growth of the endochondral skeleton. The fact that our patients with a *GNPNAT1* missense variant had a severe skeletal disorder and survived until adulthood while knocking out orthologues of *GNPNAT1*cause lethality in mice and yeast, may imply that the variant identified in our family could lead to production of GNPNAT1 which is partially functional. Further studies including generation of conditional knockout and hypomorphic animal models are necessary to elucidate the exact role of GNPNAT1 in cartilage and bone

development, cell proliferation and skeletogenesis. Additional patient reports are needed to delineate in more detail the clinical course and characteristics of this novel form of skeletal dysplasia.

Acknowledgments

We thank the family NAD-07 for participating in the study. We are grateful to Dr. Thomas Friedman for reviewing the manuscript. NA was supported by International Research Support Program (IRSP) provided by HEC, Pakistan. MB was supported by a scholarship from The Foundation Blanceflor Boncompagni Ludovisi, née Bild. ON and MB were supported by grants from the Swedish Research Council (project K2015–54X-22 736–01–4 & 2015-02227), the Swedish Governmental Agency for Innovation Systems (Vinnova) (2014-01438), Marianne and Marcus Wallenberg Foundation, IngaBritt och Arne Lundbergs forskningsstiftelse, Byggmästare Olle Engkvist Stiftelse, Nyckelfonden, Stiftelsen Frimurare Barnhuset i Stockholm, the Stockholm County Council, Karolinska Institutet, Stockholm, Sweden, and Örebro University, Örebro, Sweden. Research of OM was funded by Swedish Research Council, Academy of Finland, Sigrid Jusélius Foundation and Novo Nordisk Foundation grant and that of SN was supported by Koshish foundation USA.

Contributors

SN and OM designed and supervised the study. TI and NA collected the family samples and arranged clinical testing. NA analyzed genome sequencing data and performed Sanger sequencing. AC and FT analyzed data. MB and NA performed and analyzed knockdown experiments. ON

supervised knockdown experiments. OM and ON reviewed clinical data. NA, OM and SN wrote the manuscript. All authors reviewed and approved the manuscript.

References

1. Bonafe L, Cormier-Daire V, Hall C, Lachman R, Mortier G, Mundlos S, Nishimura G, Sangiorgi L, Savarirayan R, Sillence D. Nosology and classification of genetic skeletal disorders: 2015 revision. Am J Med Genet A 2015;**167**(12):2869-92

2. Stanley P. Golgi glycosylation. Cold Spring Harb Perspect Biol 2011;**3**(4):a005199

3. Scott K, Gadomski T, Kozicz T, Morava E. Congenital disorders of glycosylation: new defects and still counting. J Inherited Metab Dis 2014;**37**(4):609-17

4. Ng BG, Freeze HH. Perspectives on Glycosylation and Its Congenital Disorders. Trends in genetics : TIG 2018;**34**(6):466-76

5. Coman D, Irving M, Kannu P, Jaeken J, Savarirayan R. The skeletal manifestations of the congenital disorders of glycosylation. Clin Genet 2008;**73**(6):507-15

6. Li H, Durbin R. Fast and accurate short read alignment with Burrows-Wheeler transform. Bioinformatics 2009;**25**(14):1754-60

7. Van der Auwera GA, Carneiro MO, Hartl C, Poplin R, Del Angel G, Levy-Moonshine A, Jordan T, Shakir K, Roazen D, Thibault J. From FastQ data to high-confidence variant calls: the genome analysis toolkit best practices pipeline. Current protocols in bioinformatics 2013;**43**(1):11.10. 1-11.10. 33

8. McLaren W, Gil L, Hunt SE, Riat HS, Ritchie GR, Thormann A, Flicek P, Cunningham F. The ensembl variant effect predictor. Genome Biol 2016;**17**(1):122

9. Paila U, Chapman BA, Kirchner R, Quinlan AR. GEMINI: integrative exploration of genetic variation and genome annotations. PLoS Comp Biol 2013;**9**(7):e1003153

10. Spath SS, Andrade AC, Chau M, Baroncelli M, Nilsson O. Evidence That Rat Chondrocytes Can Differentiate Into Perichondrial Cells. JBMR Plus 2018;**2**(6):351-61

11. Lui JC, Garrison P, Nguyen Q, Ad M, Keembiyehetty C, Chen W, Jee YH, Landman E, Nilsson O, Barnes KM, Baron J. EZH1 and EZH2 promote skeletal growth by repressing inhibitors of chondrocyte proliferation and hypertrophy. Nat Commun 2016;**7**:13685

12. Nilsson O, Parker EA, Hegde A, Chau M, Barnes KM, Baron J. Gradients in bone morphogenetic protein-related gene expression across the growth plate. J Endocrinol 2007;**193**(1):75-84

13. Dennis JW. Glucosamine-6 Phosphate N-Acetyltransferase (GNPNAT1/GNA1). Handbook of Glycosyltransferases and Related Genes 2014:1481-88

14. Mio T, Yamada-Okabe T, Arisawa M, Yamada-Okabe H. Saccharomyces cerevisiae GNA1, an essential gene encoding a novel acetyltransferase involved in UDP-N-acetylglucosamine synthesis. J Biol Chem 1999;**274**(1):424-29

15. Boehmelt G, Wakeham A, Elia A, Sasaki T, Plyte S, Potter J, Yang Y, Tsang E, Ruland J, Iscove NN. Decreased UDP-GlcNAc levels abrogate proliferation control in EMeg32-deficient cells. The EMBO journal 2000;**19**(19):5092-104

16. Stray-Pedersen A, Backe PH, Sorte HS, Mørkrid L, Chokshi NY, Erichsen HC, Gambin T, Elgstøen KB, Bjørås M, Wlodarski MW. PGM3 mutations cause a congenital disorder of glycosylation with severe immunodeficiency and skeletal dysplasia. The American Journal of Human Genetics 2014;**95**(1):96-107

17. Campos-Xavier AB, Martinet D, Bateman J, Belluoccio D, Rowley L, Tan TY, Baxová A, Gustavson K-H, Borochowitz ZU, Innes AM. Mutations in the heparan-sulfate

proteoglycan glypican 6 (GPC6) impair endochondral ossification and cause recessive omodysplasia. The American Journal of Human Genetics 2009;**84**(6):760-70

18. Damar Ç, Boyunağa Ö, Derinkuyu BE, Battaloğlu N, Ezgü FS. Radiologic findings of Patterson-Lowry rhizomelic dysplasia in two sisters. Skeletal Radiol 2014;**43**(11):1651-54

19. Patterson C, Lowry RB. A new dwarfing syndrome with extreme shortening of humeri and severe coxa vara. Radiology 1975;**114**(2):341-42

20. Franceschini P, Licata D, Guala A, Ingrosso G, Di Cara G, Franceschini D. Patterson–Lowry rhizomelic dysplasia: Report of two new patients. Am J Med Genet A 2004;**127**(1):86-92

21. Kamoda T, Nakajima R, Matsui A, Nishimura G. Patterson-Lowry rhizomelic dysplasia: a potentially lethal bone dysplasia? Pediatr Radiol 2001;**31**(2):81-83

Legends

Figure 1: Photographs of the affected individuals IV:4 and IV:5.

A. Photograph of IV:4 showing disproportionate short stature with rhizomelia and relative macrocephaly, normal facial features, long arms and large hands relative to body length, and very short forearms (arrow). **B.** Photographs of IV:5 showing short forearms (arrow) and irregular length of metacarpal bones and shortness of the 4th metacarpal (arrow). **C.** IV:5 also has mild lower leg varus deformity and long arms and large feet relative to total height. **D.** Photograph of the feet of IV:4 showing irregular metatarsal bone length bilaterally (arrows) leading to overlapping toes.

Figure 2: Radiographs of individual IV:4 at 50 years**.**

A. Radiograph of the chest shows severe platyspondyly. **B.** All lumbar vertebrae are similarly flat and show significant degenerative changes **C**. A lateral image of the thoracic and lumbar spine shows that platyspondyly involves all vertebrae. **D.** Radiographs of the arms show shortening of the humeri bilaterally with underdeveloped proximal humerus (arrows). The radius and ulna appear normal in length and shape. **E.** Similarly, the femur is short, and the proximal femoral head is underdeveloped. Distal femur is abnormally wide **F.** A closer view of the left hip showing abnormal shapes of the proximal femur and the acetabulum.

Figure 3: Family NAD-07 and segregation of *GNPNAT1* variant.

A. Pedigree of family NAD-07. Consanguinity is indicated by double lines, filled symbols denote homozygous affected individuals and symbols with dots denote the heterozygous carriers of the variant. Asterisk (*) denotes the individuals who have been screened by WGS. Genotypes for *GNPNAT1* variant c.226G>A are given for all participants below their symbols. **B.** Partial chromatograms showing the mutation site of *GNPNAT1*. Arrows indicate the point of mutation.

Figure 4: Knockdown of *Gnpnat1* reduces proliferation of rat primary chondrocytes and induces dedifferentiation.

A. Expression of *Gnpnat1* was significantly reduced upon transfection with two siRNAs (siR1 and siR2) against *Gnpnat1*.**B.** Proliferation of rat primary chondrocytes upon transfection with siRNAs was significantly reduced as measured by BrdU incorporation. **C.** Knockdown of *Gnpnat1* by transfection with either of two siRNAs did not affect apoptosis in rat primary chondrocytes. **D.** *Alpl* expression as well as (E) *Col2a1* expression was significantly reduced upon transfection with either of the siRNAs. All measurements are performed 48h post end transfection. Bars indicate Average ± SEM of two independent experiments (*, $p<0.05$; **, $p<0.01$; ***, $p<0.001$ relative to scrambled-treated cells).

Figure 5: Amino acid conservation and schematic representation of GNPNAT1.

A. Clustal Omega multiple sequence alignment of GNPNAT1 from diverse vertebrate species showing conservation of Glutamic acid at position 76 in all orthologues. The conserved amino acids are highlighted in yellow. The asterisk signs below the alignment represent evolutionary conserved amino acids, the colon indicates an highly conserved amino acid, and the periods symbolize less conserved amino acid. **B.** Graphical representation of GNPNAT1, in which the grey area indicates the acetyltransferase domain. Amino acids are numbered with integers and the genetic variant is marked.

Table 1: Phenotypic features of NAD-07 family members.

Individual	Age	Sex	Zygosity	Height (cm)	SD	Head Circumference (cm)	Head Circumference SDS	Cognition	Gait	Speech
III:1	80	F	Heterozygous	155	-1.3	NA	NA	Normal	Normal	Normal
IV:1	48	M	Homozygous	109	-9.4	58	+2.0	Normal	Abnormal	Normal
IV:4	50	M	Homozygous	104	-10.1	58	+2.0	Normal	Abnormal	Normal
IV:5	45	F	Homozygous	99	-9.9	56	+1.5	Normal	Abnormal	Normal
IV:6	46	F	Homozygous	114	-7.6	53	-1.3	Normal	Abnormal	Normal
V:1	22	F	Wild type	154	-1.4	-	-	Normal	Normal	Normal

cm: centimeters, SD: standard deviation score. NA, not available

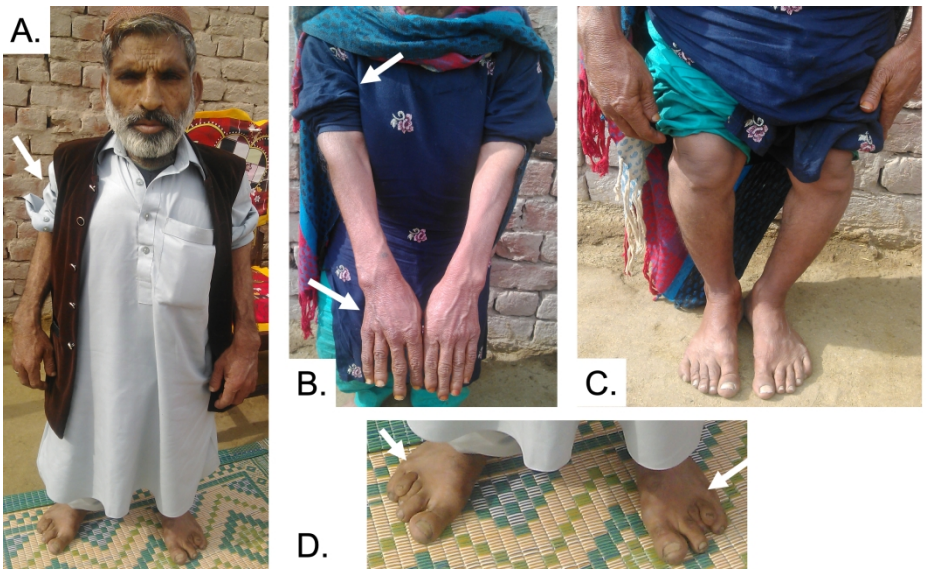

Figure 1: Photographs of the affected individuals IV:4 and IV:5.
A. Photograph of IV:4 showing disproportionate short stature with rhizomelia and relative macrocephaly, normal facial features, long arms and large hands relative to body length, and very short forearms (arrow). B. Photographs of IV:5 showing short forearms (arrow) and irregular length of metacarpal bones and shortness of the 4th metacarpal (arrow). C. IV:5 also has mild lower leg varus deformity and long arms and large feet relative to total height. D. Photograph of the feet of IV:4 showing irregular metatarsal bone length bilaterally (arrows) leading to overlapping toes.

237x133mm (300 x 300 DPI)

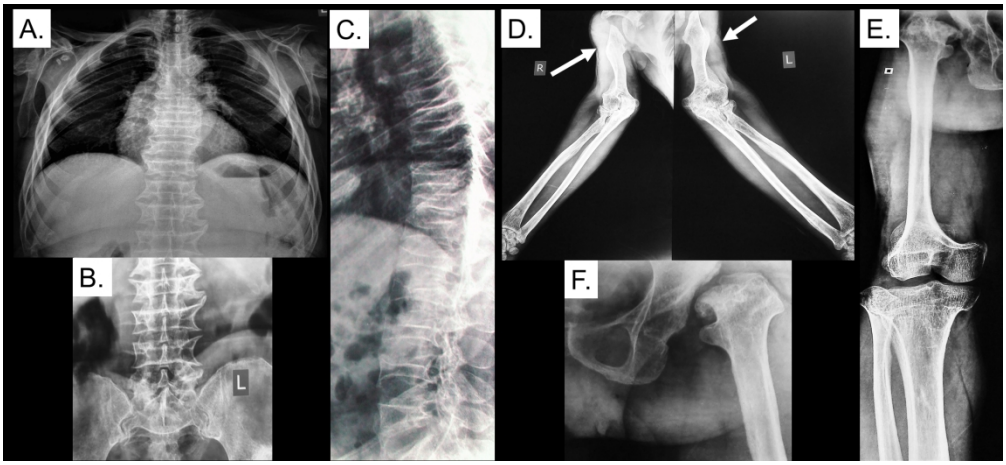

Figure 2: Radiographs of individual IV:4 at 50 years.
A. Radiograph of the chest shows severe platyspondyly. B. All lumbar vertebrae are similarly flat and show significant degenerative changes C. A lateral image of the thoracic and lumbar spine shows that platyspondyly involves all vertebrae. D. Radiographs of the arms show shortening of the humeri bilaterally with underdeveloped proximal humerus (arrows). The radius and ulna appear normal in length and shape. E. Similarly, the femur is short, and the proximal femoral head is underdeveloped. Distal femur is abnormally wide F. A closer view of the left hip showing abnormal shapes of the proximal femur and the acetabulum.

211x96mm (300 x 300 DPI)

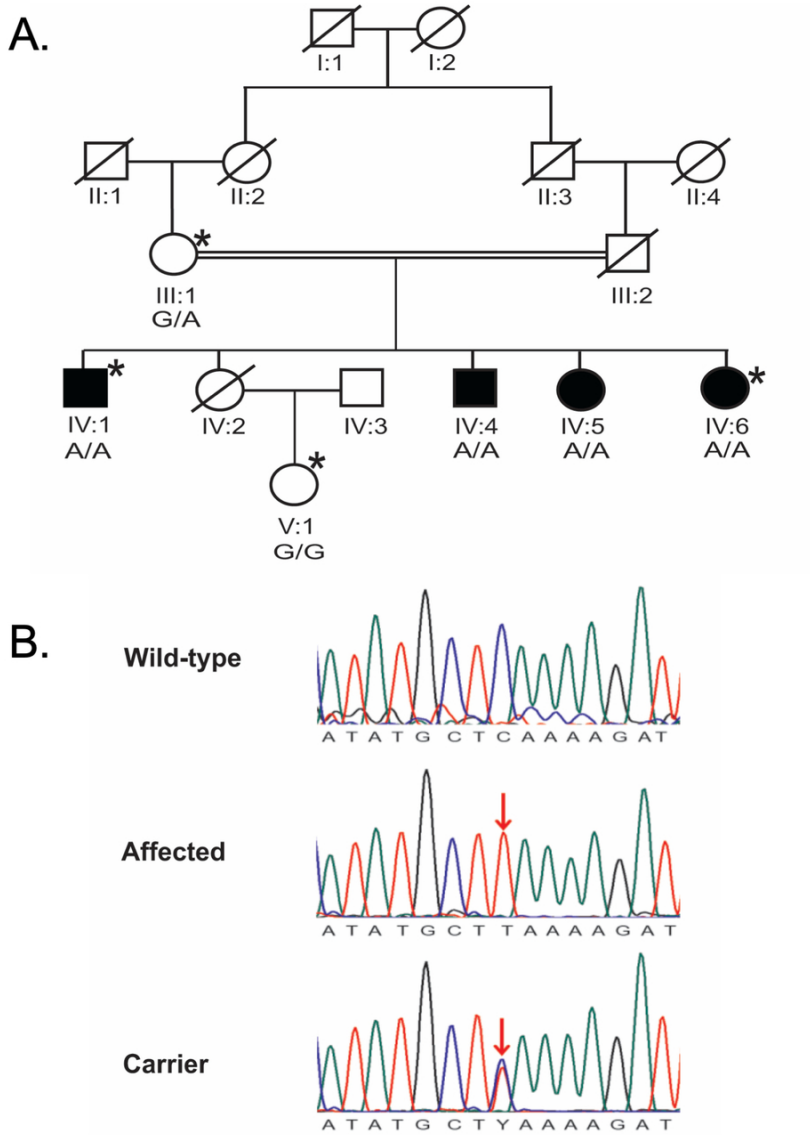

Figure 3: Family NAD-07 and segregation of GNPNAT1 variant.
A. Pedigree of family NAD-07. Consanguinity is indicated by double lines, filled symbols denote homozygous affected individuals and symbols with dots denote the heterozygous carriers of the variant. Asterisk (*) denotes the individuals who have been screened by WGS. Genotypes for GNPNAT1 variant c.226G>A are given for all participants below their symbols. B. Partial chromatograms showing the mutation site of GNPNAT1. Arrows indicate the point of mutation.

85x114mm (300 x 300 DPI)

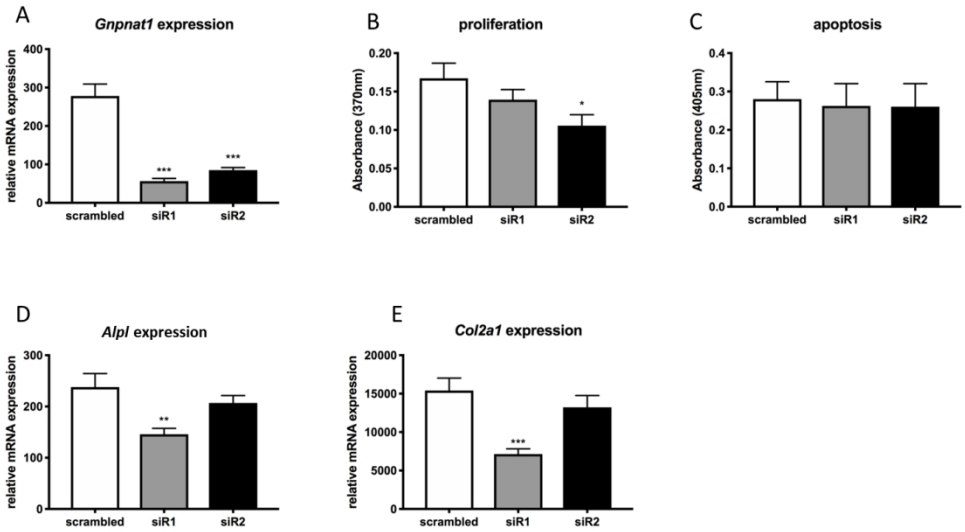

Figure 4: Knockdown of Gnpnat1 reduces proliferation of rat primary chondrocytes and induces dedifferentiation.
A. Expression of Gnpnat1 was significantly reduced upon transfection with two siRNAs (siR1 and siR2) against Gnpnat1.B. Proliferation of rat primary chondrocytes upon transfection with siRNAs was significantly reduced as measured by BrdU incorporation. C. Knockdown of Gnpnat1 by transfection with either of two siRNAs did not affect apoptosis in rat primary chondrocytes. D. Alpl expression as well as (E) Col2a1 expression was significantly reduced upon transfection with either of the siRNAs. All measurements are performed 48h post end transfection. Bars indicate Average ± SEM of two independent experiments (*, $p<0.05$; **, $p<0.01$; ***, $p<0.001$ relative to scrambled-treated cells).

127x69mm (300 x 300 DPI)

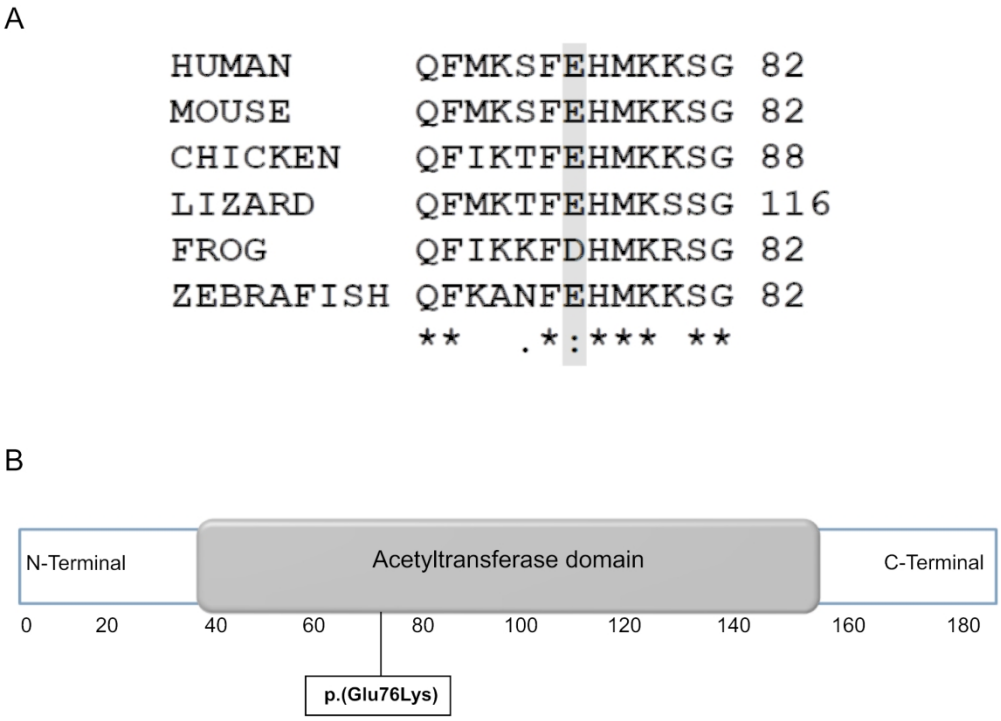

Figure 5: Amino acid conservation and schematic representation of GNPNAT1.
A. Clustal Omega multiple sequence alignment of GNPNAT1 from diverse vertebrate species showing conservation of Glutamic acid at position 76 in all orthologues. The conserved amino acids are highlighted in yellow. The asterisk signs below the alignment represent evolutionary conserved amino acids, the colon indicates an highly conserved amino acid, and the periods symbolize less conserved amino acid. B. Graphical representation of GNPNAT1, in which the grey area indicates the acetyltransferase domain. Amino acids are numbered with integers and the genetic variant is marked.

165x119mm (300 x 300 DPI)

Table S1: Homozygous variants with MAF < 0.01 identified after the analysis of WGS data.

Chr	Position[a]	Reference sequence	Altered Sequence	Gene	Transcript	Exonic	ExAC	Conserved	CADD score
1	11838347	CAAA	C	*RP11-56N19.5*	ENST00000376620	No	0	No	None
2	43025347	C	CTTTTTTT	*FTOP1*	ENST00000419363	No	0	No	None
2	154064574	ATTTTTTTTTTTTTTTTAAAAGGACATGAGGATGATTTATTTGGCAGTCAGATCTTAAGAGGGCAGCAGAACTAGCAAATGGCCAACCCTGAGCCCAAATG	A	*AC079150.2*	ENST00000443733	No	0	No	None
5	127292615	G	GAAAAAA	*CTC-228N24.3*	ENST00000499346	No	0	No	None
8	93899101	TACCATTTTTTGCC	T	*CTD-3239E11.2*	ENST00000523197	No	0	No	None
8	118019218	TTTTTC	T	*SLC30A8*	ENST00000521035	No	0	No	None
9	674384	T	A	*RP11-130C19.3*	ENST00000421645	No	0	No	3.53

9	37767509	C	A	*EXOSC3*	ENST00000465229	No	0	No	0.02
14	39308411	G	GA	*LINC00639*	ENST00000553932	No	0	No	None
14	45366778	G	A	*C14orf28*	ENST00000325192	No	0	Yes	13.83
14	53248620	C	T	*GNPNAT1*	ENST00000216410	Yes	0	Yes	22.9
15	73633409	GGTGT	G	*RP11-272D12.1*	ENST00000558742	No	0	No	None
15	75933564	CA	C	*IMP3*	ENST00000565349	No	0	No	None
15	76602408	CAAAAAAAAA	C	*ETFA*	ENST00000560044	No	0	No	None
17	61198173	CAA	C	*RP11-556O9.2*	ENST00000582889	No	0	No	None
18	2977188	CA	C	*LPIN2*	ENST00000581568	No	0	No	None
18	6926563	C	CAAAAAAA	*LINC00668*	ENST00000578278	No	0	No	None
19	1583385	CA	C	*MBD3*	ENST00000585903	No	0	No	None
19	15087848	GAAAAA	G	*SLC1A6*	ENST00000601761	No	0	No	None
19	2015539	GGGC	G	*BTBD2*	ENST00000255608	Yes	0	No	None
X	27765398	AGAG	A	*DCAF8L2*	ENST00000451261	Yes	0	No	None

[a] positions are according to human UCSC Genome Browser Feb. 2009 (GRCh37/hg19)